arXiv:cond-mat/0502115v1 [cond-mat.mtrl-sci] 4 Feb 2005

Antiferromagnetic $s-d$ exchange coupling in GaMnAs

R. C. Myers, M. Poggio, N. P. Stern, A. C. Gossard, and D. D. Awschalom
Center for Spintronics and Quantum Computation,
University of California, Santa Barbara, CA 93106
(Dated: March 23, 2022)

Measurements of coherent electron spin dynamics in $Ga_{1-x}Mn_xAs/Al_{0.4}Ga_{0.6}As$ quantum wells with $0.0006\% < x < 0.03\%$ show an antiferromagnetic (negative) exchange bewteen s-like conduction band electrons and electrons localized in the d-shell of the Mn^{2+} impurities. The magnitude of the $s-d$ exchange parameter, $N_0\alpha$, varies as a function of well width indicative of a large and negative contribution due to kinetic exchange. In the limit of no quantum confinement, $N_0\alpha$ extrapolates to -0.09 ± 0.03 eV indicating that antiferromagnetic $s-d$ exchange is a bulk property of GaMnAs. Measurements of the polarization-resolved photoluminescence show strong discrepancy from a simple model of the exchange enhanced Zeeman splitting, indicative of additional complexity in the exchange split valence band.

PACS numbers: 75.30.Et, 71.70.Ej, 75.50.Pp, 78.47.+p

The $sp-d$ exchange constants in II-VI dilute magnetic semiconductors (DMS) are readily measurable through magneto-optical spectroscopy; however, the high concentration of growth defects in $Ga_{1-x}Mn_xAs$ ($x > 1\%$) has precluded band-edge optical measurements of its exchange splitting. Despite this constraint, several estimates of the $p-d$ exchange constant ($N_0\beta$) have been published from modeling of transport [1], core-level photoemission [2], and cyclotron resonance measurements [3]. A previous study on highly dilute $Ga_{1-x}Mn_xAs$ ($x < 0.1\%$) crystals grown by the Czochralski method reports polarized magnetoreflectance data from which the total exciton spin splitting is determined to within 600 meV [4]. This result, however, includes no independent measurements of the $s-d$ exchange constant ($N_0\alpha$) or $N_0\beta$; the reported estimation of $N_0\beta$ depends on an assumed positive value of $N_0\alpha$ based on work in II-VI DMS.

Here we investigate MBE grown $Ga_{1-x}Mn_xAs/Al_{0.4}Ga_{0.6}As$ quantum wells (QWs) with $0.0006\% < x < 0.03\%$ in which Mn^{2+} ions act as spin 5/2 paramagnets. $Ga_{1-x}Mn_xAs$ is typically grown at temperatures around 250°C, however, for these values of x, the growth temperature can be increased to 400°C while still allowing substitutional incorporation of Mn. The use of this increased substrate temperature is seen to reduce excess As in our samples and enables the observation of magneto-optical effects such as polarization resolved photoluminescence (PL) and Kerr rotation (KR) [5]. Both the sign and magnitude of $N_0\alpha$ are measured over a wide range of QW widths and Mn concentrations by time-resolved measurements of KR. In contrast to II-VI DMS, we find that $N_0\alpha < 0$ in all QWs measured. A measured negative trend in $N_0\alpha$ as a function of decreasing QW width is consistent with the mechanism of kinetic exchange for conduction band electrons observed in II-VI DMS QWs [6]. Using a fit to this model in the limit of wide wells, we extrapolate a negative $N_0\alpha$ for bulk GaMnAs. The change in $N_0\alpha$ due to quantum confinement is as large as -740 meV, much larger than observed by Merkulov *et al.* in II-VI DMS. Measurements of polarization-resolved PL reveal strong non-linearities in the Zeeman splitting, making it difficult to extract the exchange-induced exciton energy $N_0(\alpha-\beta)$, and thus $N_0\beta$.

The samples consist of single $Ga_{1-x}Mn_xAs$ QWs of width d surrounded by $Al_{0.4}Ga_{0.6}As$ barriers and are grown on (001) semi-insulating GaAs wafers. A detailed discussion of sample growth and quantitative measurements of x by secondary ion mass spectroscopy are provided elsewhere [5].

Electron spin dynamics are measured by time-resolved KR with the optical axis perpendicular to the applied magnetic field B (Voigt geometry) and parallel to the growth direction $\hat{z}$. The measurement, which monitors small rotations in the linear polarization of laser light reflected off of the sample, is sensitive to the spin polarization of electrons in the conduction band of the QW [7]. A Ti:Sapphire laser with a 76-MHz repetition rate and 250-fs pulse width tuned to a laser energy E_L near the QW absorbtion energy is split into a pump (probe) beam with an average power of 2 mW (0.1 mW). The helicity of the pump beam polarization is modulated at 40 kHz by a photo-elastic modulator, while the intensity of the linearly polarized probe beam is modulated by an optical chopper at 1 kHz for lock-in detection. Both beams are focused to an overlapping 50 μm diameter spot on the sample which is mounted within a magneto-optical cryostat. The time delay Δt between pump and probe pulses is controlled using a mechanical delay line. The pump injects electron spins polarized perpendicular to B into the conduction band of the QW. The change in the probe polarization angle, $\theta_K(\Delta t)$ is proportional to the average electron spin polarization in the QW and is well fit to a single decaying cosine, $\theta_K(\Delta t) = \theta_\perp e^{-\Delta t/T_2^*}\cos(2\pi\nu_L\Delta t + \phi)$, where $\theta_\perp$ is proportional to the total spin injected, T_2^* is the inhomo-

geneous transverse spin lifetime, ν_L is the electron spin precession (Larmor) frequency, and ϕ is the phase offset. No evidence of Mn^{2+} spin precession, which occurs in II-VI magnetically doped QWs [7], has been observed in the samples studied here. The order of magnitude smaller x in our III-V QWs compared to the II-VI QWs puts any Mn^{2+} spin precession signal below the experimental detection limit.

Fig. 1a shows typical time-resolved KR data measured at $B = 8$ T for a Mn-doped QW ($d = 7.5$ nm and $x \sim 0.01\%$) together with fit, as described above, demonstrating electron spin coherence in the GaMnAs system. ν_L is proportional to the total conduction band spin splitting between spin-up and spin-down electrons ($\Delta E = E\uparrow - E\downarrow$) and can be expressed in terms of the Zeeman splitting (ΔE_g), and the $s-d$ exchange splitting (ΔE_{s-d}):

$$h\nu_L = \Delta E = \Delta E_g + \Delta E_{s-d} = g_e\mu_B B - xN_0\alpha\langle S_x\rangle. \quad (1)$$

Here h is Planck's constant, g_e is the in-plane electron g-factor, μ_B is the Bohr magneton, and $\langle S_x\rangle$ is the component of Mn^{2+} spin along B. We emphasize that a measurement of ν_L alone, because of phase ambiguity, does not determine the sign of ΔE. $\langle S_x\rangle = -\frac{5}{2}B_{5/2}\left(\frac{5g_{Mn}\mu_B B}{2k_B(T-\theta_P)}\right)$, where $B_{5/2}$ is the spin-5/2 Brillouin function, g_{Mn} is the g-factor for Mn^{2+}, k_B is Boltzman's constant, and θ_P is the paramagnetic Curie temperature. Note that since the g-factor for Mn^{2+} ($g_{Mn} = 2$) is positive, then for $B > 0$, $\langle S_x\rangle < 0$.

In Fig. 1b, ν_L is plotted as a function of B for a set of four samples with $d = 7.5$ nm and varying x. The non-magnetic ($x = 0$) sample shows a linear field dependence of ν_L, from which we extract values of g_e as described in Eq. (1). As the Mn doping concentration is increased, ν_L increases and its B dependence becomes non-linear. Further, this field dependence shows the same Brillouin function behavior that is expected for the magnetization of paramagnetic GaMnAs, Eq. (1).

The dependence of ν_L on B and T for the sample with $d = 7.5$ nm and $x \sim 0.002\%$ is plotted in Fig. 1c and d together with values for the control sample, $x = 0$ and $d = 7.5$ nm. For the magnetic sample, as T is increased ν_L decreases asymptotically toward the control sample value $g_e\mu_B B/h$ without crossing zero (Fig. 1c). Thus, it follows from Eq. (1) and from the sign of $\langle S_x\rangle$ that for $d = 7.5$ nm $N_0\alpha$ has the same sign as g_e. For $d = 7.5$ nm, $g_e < 0$ [9], and thus $N_0\alpha < 0$. This conclusion is also supported by the QW width dependence discussed below.

Using g_e extracted from the $x = 0$ sample (green line) and Eq. (1) we fit ν_L as a function of B and T to,

$$\nu_L = \frac{g_e\mu_B B}{h} + \frac{5A}{2h}B_{5/2}\left(\frac{5\mu_B B}{k_B(T-\theta_P)}\right), \quad (2)$$

which has only two fit parameters, A and θ_P. Comparing Eqs. (2) to (1), it is clear that $A = xN_0\alpha$. The data in Fig. 1b-d are fit to Eq. (2), with fits shown as red lines. A large negative θ_P (-37 K) is extracted from the fits for the sample with the lowest Mn doping (Fig.1c and d), which may be explained by an increased spin temperature of Mn^{2+} due to photoexcitation. This effect has been reported in II-VI DMS for low magnetic doping levels [8]. Also supporting this hypothesis, we find smaller values of $|\theta_P| < 7$ K in samples with larger x.

$N_0\alpha$ is examined in detail for QWs of varying d. For this analysis, four sets of samples with various x (including $x = 0$) were grown for $d = 3, 5, 7.5$ and 10 nm. Note that each sample set of constant d was grown on the same day, which we have observed to reduce QW thickness variations between samples within each set from $\sim 3\%$ to $< 1\%$. In Fig. 2a, g_e in the non-magnetic ($x = 0$) QWs is plotted as a function of d together with data from two other publications [9, 10]. Our data track the thickness dependence of the QW g-factor as previously reported with a slight positive shift in g_e. The larger Al concentration (40%) in the QW barriers used in our samples versus the concentration (33%) used in Refs. [9, 10] accounts for this discrepancy [11]. Knowing the absolute sign of g_e for QWs of any width, we determine the sign of $N_0\alpha$ for each d in the manner described previously. With a now calibrated sign, $\Delta E = h\nu_L$ is plotted in Fig. 2b as a function of B for all four QW sample sets with varying d. As shown in Fig. 2b, for any given d, ΔE

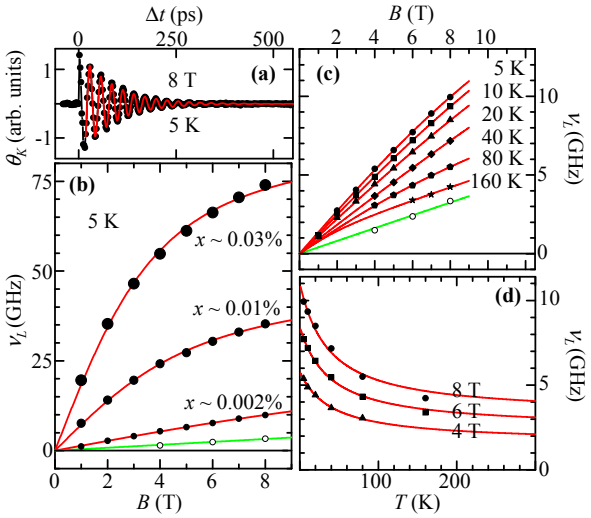


FIG. 1: (Color) Time-resolved electron spin dynamics in $d = 7.5$ nm GaMnAs QWs. (a) An example of KR data (points) together with fit (line). (b) ν_L as a function of B for different x values (solid points); larger points indicate increasing x. Open data points are for the $x = 0$ sample. (c) The effect of increasing T on the B dependence of ν_L for the sample with $x \sim 0.002\%$ (solid points) and for the $x = 0$ sample (open points). (d) T dependence of ν_L at constant B for the $x \sim 0.002\%$ sample. Red lines in (b-d) are fits to Eq. (2).

decreases as x increases. Following from Eq. (1) and from the sign of $\langle S_x \rangle$, this demonstrates that $N_0\alpha$ is negative, i.e. antiferromagnetic, which has been reproduced unambiguously in at least 20 additional samples. The effect of increasing temperature on the B dependence of ΔE for the $d = 5$ nm and $x \sim 0.008\%$ sample is shown in Fig. 2c, which dramatically illustrates the negative $s-d$ constant. For $d = 5$ nm, g_e is weakly positive, thus for $B > 0$ and at high temperature $\Delta E > 0$. As the temperature descreases, ΔE_{s-d} becomes more negative as the paramagnetic susceptibility increases. At $T = 10$ K and $B = 7$ T, $\Delta E = 0$ since the $s-d$ exchange splitting is equal and opposite to the Zeeman splitting. For lower temperature, $\Delta E < 0$ since $\Delta E_{s-d} > \Delta E_g$. We note that the data are well fit to Eq. (2) despite their highly non-linear nature. We contrast our observation of antiferromagnetic $s-d$ exchange in III-V GaMnAs, with the ferromagnetic $s-d$ exchange ubiquitous in II-VI DMS. Their symmetry forbids hybridization of s and d orbitals, such that only direct (ferromagnetic) $s-d$ exchange is possible [12]. The antiferromagnetic $s-d$ exchange in GaMnAs may be due to the narrower band gap of this material compared with II-VI, such that the conduction band has partial p-character thus allowing hybridization with the d orbitals localized on the Mn^{2+} impurities.

In Fig. 3a, the fit parameter $A = xN_0\alpha$ is plotted as a function of x together with linear fits for each sample set of constant d. The finite values of $xN_0\alpha$ at $x = 0$, extrapolated from the linear fits, are attributed to either the experimental error in the determination of g_e in the non-magnetic QWs or error in the measurement of x, both errors which to first approximation have negligible effect on the slope. These linear fits demonstrate that $N_0\alpha$ is constant over the measured doping range for QWs with the same width, but it varies with d as plotted in Fig. 3b. $N_0\alpha$ is more negative the narrower the QW, while it appears to saturate for wide QWs. In II-VI DMS QWs, a negative change in $N_0\alpha$ as large as -170 meV was previously reported for increasing confinement and was attributed to a kinetic exchange coupling due to the admixture of valence and conduction band wave functions [6]. We plot $N_0\alpha$ as a function of the electron kinetic energy (E_e) in Fig. 3c, and the data are linear. Extrapolating to $E_e = 0$ we obtain a bulk value of $N_0\alpha = -0.09 \pm 0.03$ eV for GaMnAs. A change in $N_0\alpha$ as large as -740 meV is observed in the narrrowest wells measured ($d = 3$ nm) and the slope of $N_0\alpha(E_e)$ is ~ 5 times larger than in Merkulov *et al.*

Polarization-resolved PL is measured as a function of B in the Faraday geometry with PL collected normal to the sample surface. The excitation laser is linearly polarized and focused to a spot 100 μm in diameter with an energy set above the QW absorption energy. While PL is seen to quench with increasing Mn doping, QWs without or with low Mn doping emit PL whose energy dependence is well fit by two Gaussians (Fig. 4a and b). In the non-magnetic samples, the emission energy of the narrower, higher-energy Gaussian peak tracks the B dependence expected for the Zeeman splitting in QWs, indicating that this peak is due to heavy hole exciton recombination. On the other hand, the wider, lower-energy Gaussian is likely due to donor-bound exciton emission from shallow donors in the QWs. These shallow donors are likely Mn interstitials, since the emission linewidth increases as the

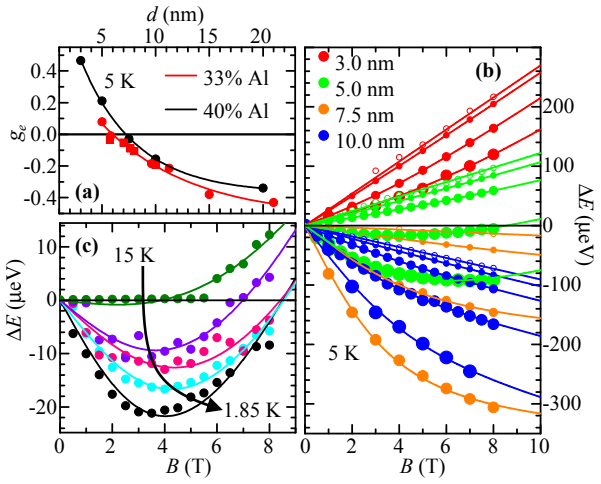


FIG. 2: (Color) (a) g_e as a function of d. Black points are from control ($x = 0$) samples of this study, red circles and squares are from references [9, 10], respectively. Lines guide the eye. (b) ΔE as a function of B for QWs with (solid circles) and without Mn doping (open circles); larger points indicate increasing x. (c) ΔE for the sample with $d = 5$ nm and $x \sim 0.008\%$ at various temperatures. Fits to Eq. (2) are shown as lines in (b) and (c).

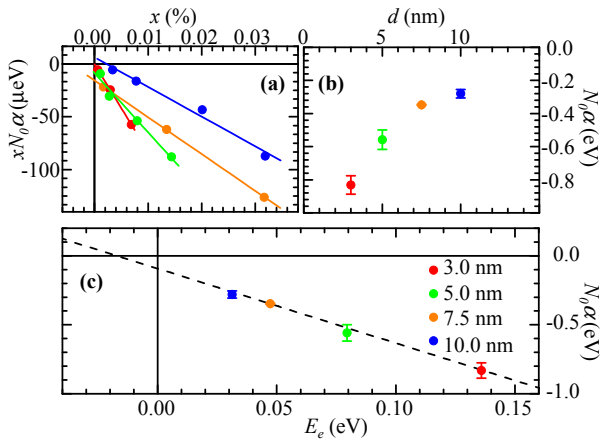


FIG. 3: (Color) (a) $xN_0\alpha$ as a function of x from fits shown in Fig. 2b; error bars are the size of the points. Linear fits are shown for each sample set of constant d. (b) $N_0\alpha$ extracted from fits in (a) and plotted as a function of d. (c) The electron exchange constant $N_0\alpha$ as a function of electron kinetic energy for GaMnAs.

calculated Mn interstitial concentration increases. The lower energy Gaussian is also present in the non-magnetic samples (Fig. 4a) perhaps due to an impurity level of Mn interstitials ($\leq 10^{15}$ cm^{-3}) [5].

The splitting in the polarized emission energy of the higher energy Gaussian, $\Delta E_{PL} = E_{\sigma^+} - E_{\sigma^-}$, is measured in all the non-magnetic samples. For small fields ($B < 2$ T), ΔE_{PL} depends linearly on field with the slope giving the out-of-plane heavy hole exciton g-factor (g_{ex}). The extracted values of g_{ex} agree within the experimental error with previously published values [13]. At higher fields, ΔE_{PL} deviates from linearity, particularly in the wider QWs as shown in Fig. 4c where it reverses sign in the 10 nm QW with $x = 0$ at $|B| = 5$ T.

In Mn-doped samples, ΔE_{PL} results from both the Zeeman splitting (ΔE_{gex}) and the $sp-d$ exchange splitting (ΔE_{sp-d}):

$$\Delta E_{PL} = \Delta E_{gex} + \Delta E_{sp-d} = -g_{ex}\mu_B B + xN_0(\alpha - \beta)\langle S_x \rangle. \quad (3)$$

Using the measurements of g_{ex} from the $x = 0$ samples and the previously extracted values of $\langle S_x \rangle$ and $N_0\alpha$ at 5K (Fig. 2b), we fit ΔE_{PL} to Eq. (3). In the 10 nm QW for low fields we estimate $N_0\beta = -3.4 \pm 1.5$ eV using the fits shown in Fig. 4c as blue lines. As Fig. 4c makes clear, this model breaks down at high fields where non-linearities dominate ΔE_{PL}. In an attempt to avoid non-linearities in the Zeeman splitting not modeled by a linear ΔE_{gex}, ΔE_{PL} measured in the 10 nm $x = 0$ sample is subtracted from ΔE_{PL} of the 10 nm $x \sim 0.003\%$ sample. The resulting energy, ΔE_{sp-d}, isolates the exchange splitting, plotted as a function of B in Fig. 4d along with a fit of the form $xN_0(\alpha - \beta)\langle S_x \rangle$. While a fit giving $N_0\beta = -3.5 \pm 1.5$ eV closely approximates the data for $|B| < 5$ T, the description breaks down at larger B.

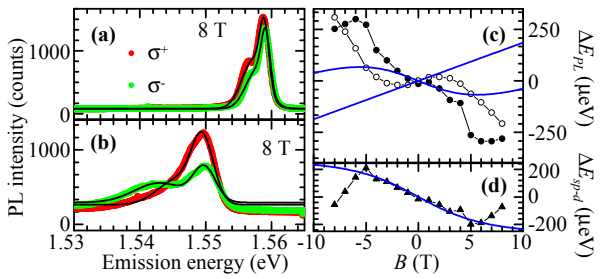


FIG. 4: (Color) Polarization-resolved PL for 10 nm QW at 5 K. (a) σ^+ and σ^- polarized PL from the $x = 0$ QW excited with 1 W/cm^2 at 1.722 eV. 2-Gaussian fits to the data are shown as black lines and the higher energy Gausssian is attributed to the heavy hole exciton in the QW. (b) Similar data shown for the $x \sim 0.003\%$ sample excited with 10 W/cm^2 at 1.722 eV. (c) B dependence of ΔE_{PL} for the $x = 0$ and $x \sim 0.003\%$ samples plotted as open and filled circles, respectively. Fits to ΔE_{PL} for $|B| < 2$ T are shown for both samples as blue lines. (d) The difference between ΔE_{PL} in the $x \sim 0.003\%$ sample and in the $x = 0$ sample, ΔE_{sp-d}, (black triangles) plotted with fit for $|B| < 5$ T (blue line).

Similar non-linear behavior in ΔE_{PL} at high fields in samples with $d = 3$, 5, and 7.5 nm gives a large uncertainty in our estimates of $N_0\beta$. Further complicating the determination of $N_0\beta$ are the widely differing values extracted for samples of different widths. Using fits similar to those shown in Fig. 4c we find $N_0\beta = +17.7 \pm 1.6$, $+98.0 \pm 7.3$, and -11.5 ± 6.1 eV for QWs with $d = 3$, 5, and 7.5 nm, respectively. Such dissagreement between samples indicates the incompleteness of our model for the valance band; the mixing of valance band states may be contributing to the problematic extraction of the $p - d$ exchange coupling especially for small d [13]. Clearly, more work is necessary for the determination of $N_0\beta$ in GaMnAs QWs and its dependence on d.

In summary, strong evidence is presented of a direct relation between the conduction band exchange constant and the electron kinetic energy due to one-dimensional quantum confinement in GaMnAs QWs. It is a quantitatively larger effect, but with the same sign, as what was reported for II-VI DMS QWs [6]. Surprisingly, the $s - d$ exchange coupling is antiferromagnetic in the QWs and extrapolates to -0.09 ± 0.03 eV in the limit of infinitely wide wells indicating that antiferromagnetic $s - d$ exchange is a bulk property of GaMnAs, a result which has not been predicted by current DMS theories.

This work was supported by DARPA, ONR, and NSF. One of us (N.P.S.) acknowledges support from the Fannie and John Hertz Foundation.

[1] F. Matsukura, H. Ohno, A. Shen, and Y. Sugawara, Phys. Rev. B **57**, 2037(R) (1998).
[2] J. Okabayashia, A. Kimura, O. Rader, T. Mizokawa, A. Fujimori, T. Hayashi, and M. Tanaka, Phys. Rev. B **58**, R4211 (1998).
[3] M. A. Zudov, J. Kono, Y. H. Matsuda, T. Ikaida, N. Miura, H. Munekata, G. D. Sanders, Y. Sun, and C. J. Stanton, Phys. Rev. B **66**, 161307(R) (2002).
[4] J. Szczytko, W. Mac, A Stachow, A Twardowski, P. Becla, and J. Tworzydlo, Solid State Commun. **99**, 927 (1996).
[5] M. Poggio, R. C. Myers, N. P. Stern, A. C. Gossard, and D. D. Awschalom (in preparation).
[6] I. A. Merkulov, D. R. Yakovlev, A. Keller, W. Ossau, J. Heurts, A. Waag, G. Landwehr, G. Karczewski, T. Wojtowicz, and J. Kossut, Phys. Rev. B **83**, 1431 (1999).
[7] S. A. Crooker, D. D. Awschalom, J. J. Baumberg, F. Flack, and N. Samarth Phys. Rev. B **56**, 7574 (1997); S. A. Crooker, J. J. Baumberg, F. Flack, N. Samarth, D. D. Awschalom, Phys. Rev. Lett. **77**, 2814 (1996).
[8] D. Keller, D. R. Yakovlev, B. Konig, W. Ossau, Th. Gruber, A. Waag, and L. W. Molenkamp, Phys. Rev. B **65**, 035313 (2001).
[9] M. J. Snelling, G. P. Flinn, A. S. Plaut, R. T. Harley, A. C. Tropper, R. Eccleston, and C. C. Phillips, Phys. Rev.

B **44**, 11345 (1991).
[10] M. Poggio, G. M. Steeves, R. C. Myers, N. P. Stern, A. C. Gossard, and D. D. Awschalom, Phys. Rev. B **70**, 121305(R) (2004).
[11] C. Weisbuch and C. Hermann, Phys. Rev. B **15**, 816 (1977).
[12] B. E. Larson, K. C. Hass, H. Ehrenreich, and A. E. Carlsson, Phys. Rev. B **37**, 4137 (1988).
[13] M. J. Snelling, E. Blackwood, C. J. McDonagh, and R. T. Harley, Phys. Rev. B **45**, 3922 (1992).